Oxygen Transport Ceramic Membranes

Quarterly Report

January 2003 – March 2003

Principal Authors:

Prof. S. Bandopadhyay

Dr. N. Nagabhushana

Issued: August 07, 2003

DOE Award # DE-FC26-99FT40054

**School of Mineral Engineering,
University of Alaska Fairbanks
Fairbanks, AK 99775**

Contributing sub contractors:

1. **Prof. Thomas W. Eagar, Dr. Harold R Larson, Mr. Raymundo Arroyave**; Massachusetts Institute of Technology, Department of Materials Science and Engineering, Cambridge, Massachusetts 02139

2. **Prof. Harlan Anderson, Dr. Wayne Huebner, Dr. Xiao-Dong Zhou**; Materials Research Center, University of Missouri-Rolla, Rolla, MO 65401

3. **Prof. Nigel Browning;** Department of Chemical Engineering and Materials Science, University of California-Davis, One Shields Ave, Davis, CA 95616

4. **Prof. Alan Jacobson and Prof. C.A. Mims** University of Houston/University of Toronto

DISCLAIMER

This report was prepared as an account of work sponsored by an agency of the United States Government. Neither the United States Government nor any agency thereof, nor any of their employees, makes any warranty, express or implied, or assumes any legal liability or responsibility for the accuracy, completeness, or usefulness of any information, apparatus, product, or process disclosed, or represents that its use would not infringe privately owned rights. Reference herein to any specific commercial product, process, or service by trade name, trademark, manufacturer, or otherwise does not necessarily constitute or imply its endorsement, recommendation, or favoring by the United States Government or any agency thereof. The views and opinions of authors expressed herein do not necessarily state or reflect those of the United States Government or any agency thereof

ABSTRACT

In the present quarter, experiments are presented on ceramic/metal interactions of Zirconia/ Ni-B-Si system and with a thin Ti coating deposited on zirconia surface. Existing facilities were modified for evaluation of environmental assisted slow crack growth and creep in flexural mode. Processing of perovskites of LSC, LSF and LSCF composition were continued for evaluation of mechanical properties as a function of environment. These studies in parallel to those on the LSFCO composition is expect to yield important information on questions such as the role of cation segregation and the stability of the perovskite structure on crack initiation vs. crack growth. Studies have been continued on the $La_{1-x}Sr_xFeO_{3-d}$ composition using neutron diffraction and TGA studies. A transition from p-type to n-type of conductor was observed at relative low pO2, at which the majority carriers changed from the holes to electrons because of the valence state decreases in Fe due to the further loss of oxygen. Investigation on the thermodynamic properties of the membrane materials are continued to develop a complete model for the membrane transport. Data obtained at 850ºC show that the stoichiometry in $La_{0.2}Sr_{0.8}Fe_{0.8}Cr_{0.2}O_{3-x}$ vary from ~2.85 to 2.6 over the pressure range studied. From the stoichiometry a lower limit of 2.6 corresponding to the reduction of all Fe^{4+} to Fe^{3+} and no reduction of Cr^{3+} is expected.

TABLE OF CONTENTS

LIST OF GRAPHICAL MATERIALS

INTRODUCTION

Conversion of natural gas to liquid fuels and chemicals is a major goal for the Nation as it enters the 21st Century. Technically robust and economically viable processes are needed to capture the value of the vast reserves of natural gas on Alaska's North Slope, and wean the Nation from dependence on foreign petroleum sources. Technologies that are emerging to fulfill this need are all based syngas as an intermediate. Syngas (a mixture of hydrogen and carbon monoxide) is a fundamental building block from which chemicals and fuels can be derived. Lower cost syngas translates directly into more cost-competitive fuels and chemicals.

The currently practiced commercial technology for making syngas is either steam methane reforming (SMR) or a two-step process involving cryogenic oxygen separation followed by natural gas partial oxidation (POX). These high-energy, capital-intensive processes do not always produce syngas at a cost that makes its derivatives competitive with current petroleum-based fuels and chemicals.

In the mid 80's BP invented a radically new technology concept that will have a major economic and energy efficiency impact on the conversion of natural gas to liquid fuels, hydrogen, and chemicals.[1] This technology, called Electropox, integrates oxygen separation with the oxidation and steam reforming of natural gas into a single process to produce syngas with an economic advantage of 30 to 50 percent over conventional technologies.[2]

The Electropox process uses novel and proprietary solid metal oxide ceramic oxygen transport membranes [OTMs], which selectively conduct both oxide ions and electrons through their lattice structure at elevated temperatures.[3] Under the influence of an oxygen partial pressure

---

[1]Mazanec, T. J.; Cable, T. L.; Frye, J. G., Jr.; US 4,793,904, 27 Dec **1988**, assigned to The Standard Oil Company (now BP America), Mazanec, T. J.; Cable, T. L.; US 4,802,958, 7 Feb **1989**, assigned to the Standard Oil Co. (now BP America), Cable, T. L.; Mazanec, T. J.; Frye, J. G., Jr.; European Patent Application 0399833, 24 May **1990**, published 28 November **1990.**

[2]Bredesen, R.; Sogge, J.; "A Technical and Economic Assessment of Membrane Reactors for Hydrogen and Syngas Production" presented at Seminar on the Ecol. Applic. of Innovative Membrane Technology in the Chemical Industry", Cetraro, Calabria, Italy, 1-4 May **1996**.

[3]Mazanec, T.J., *Interface*, **1996**; Mazanec, T.J., *Solid State Ionics*, 70/71, **1994** 11-19; "Electropox: BP's Novel Oxidation Technology", T.J. Mazanec, pp 212-225, in "The Role of Oxygen in Improving Chemical Processes", M. Fetizon and W.J. Thomas, eds, Royal Society of Chemistry, London, **1993**; "Electropox: BP's Novel Oxidation Technology", T.J. Mazanec, pp 85-96, in "The Activation of Dioxygen and Homogeneous Catalytic Oxidation", D.H.R. Barton, A. E. Martell, D.T. Sawyer, eds, Plenum Press, New York, **1993**; "Electrocatalytic Cells for

gradient, oxygen ions move through the dense, nonporous membrane lattice at high rates with 100 percent selectivity. Transported oxygen reacts with natural gas on the fuel side of the ceramic membrane in the presence of a catalyst to produce syngas.

In 1997 BP entered into an OTM Alliance with Praxair, Amoco, Statoil and Sasol to advance the Electropox technology in an industrially sponsored development program. These five companies have been joined by Phillips Petroleum and now are carrying out a multi-year $40+ million program to develop and commercialize the technology. The program targets materials, manufacturing and engineering development issues and culminates in the operation of semi-works and demonstration scale prototype units.

The Electropox process represents a truly revolutionary technology for conversion of natural gas to synthesis gas not only because it combines the three separate unit operations of oxygen separation, methane oxidation and methane steam reforming into a single step, but also because it employs a chemically active ceramic material in a fundamentally new way. On numerous fronts the commercialization of Electropox demands solutions to problems that have never before been accomplished. Basic problems in materials and catalysts, membrane fabrication, model development, and reactor engineering all need solutions to achieve commercial success.

Six important issues have been selected as needing understanding on a fundamental level at which the applied Alliance program cannot achieve the breadth and depth of understanding needed for rapid advancement. These issues include:

1. Oxygen diffusion kinetics (University of Houston);
2. Grain structure and atomic segregation (University of Illinois - Chicago);
3. Phase stability and stress development (University of Missouri - Rolla);
4. Mechanical property evaluation in thermal and chemical stress fields (University of Alaska Fairbanks);
5. Graded ceramic/metal seals (Massachusetts Institute of Technology).

Statement of Work

Task 1   Design, fabricate and evaluate ceramic to metal seals based on graded ceramic powder / metal braze joints.

Chemical Reaction", T.J. Mazanec, T.L. Cable, J.G. Frye, Jr.; Prep Petrol Div ACS, San Fran, **1992** *37*, 135-146; T.J. Mazanec, T.L. Cable, J.G. Frye, Jr.; *Solid State Ionics*, **1992**, 53-56, 111-118.

Task 2   Determine materials mechanical properties under conditions of high temperatures and reactive atmospheres.

Task 3   Evaluate phase stability and thermal expansion of candidate perovskite membranes and develop techniques to support these materials on porous metal structures.

Task 4   Assess the microstructure of membrane materials to evaluate the effects of vacancy-impurity association, defect clusters, and vacancy-dopant association on the membrane performance and stability.

Task 5   Measure kinetics of oxygen uptake and transport in ceramic membrane materials under commercially relevant conditions using isotope labeling techniques.

EXECUTIVE SUMMARY

Research on the Oxygen Transport Membranes as listed as tasks 1-5 are being performed at the various universities under the stewardship of Praxair. The progress of the various tasks were discussed at the semi-annual review meeting at University of Missouri-Rolla and the tasks redefined to better understand the fundamental concepts in the performance of the ceramic membrane.

As has been noted in other reports, the creation of reliable ceramic/metal seals between perovskite-based ceramics and nickel-based super alloys had been hindered by the observed excessive interfacial reactions between the braze alloys used and the ceramic substrate itself. Due to the high porosity of the ceramic (perovskite) substrates so far utilized, the reactions between the nickel-based brazing alloys and the ceramic substrates are usually very fast, as infiltration of the braze alloy causes the 'interfacial' reaction zone to extend tens of microns within the perovskite material. The nature of this interfacial reaction consists on the localized reduction and subsequent decomposition of the perovskite substrate and the eventual precipitation of more stable oxide phases closer to the interface with the liquid nickel-based brazing alloy. For the present study a relatively thin Ti coating was deposited on top of the zirconia substrate and a Ni-based amorphous foil was placed between the coated zirconia sample and the Ni-based super alloy. The process was designed so at a relatively high temperature, the Ti coating would react with the zirconia and produce a Ti-based oxide that could in turn be wetted by the Ni-braze. As discussed in the report, no interfacial defects were observed at the joint

In earlier studies, the strength of OTM tubes was tested in C-ring geometry. However, with the increasing complexity (Such as effect of stress distribution on degradation) in the membrane behavior, emphasis was also laid on evaluating the strength of membranes in flexure geometry. In accordance, 4 –point bend fixture were designed and fabricated. It was decided to look at the slow –crack growth behavior of the materials as a function of environment to generate a quantitative value for the degradation process on the structural properties. However, due to lack of requisite samples, initial studies are planned on Lanthanum Strontium Cobaltite and Lanthanum Strontium Ferrite. In the present quarter, the 4 –point bend fixture was fully installed and the system re configured to enable slow crack growth and creep testes. Initial test were done on standard Alumina and YSZ samples. Studies were also begun on LSCF– 8282 composition that are well studied in literature with available defect chemistry models

This interrelationship between the cation and their role in vacancy creation were studies in a model (La, Sr)(Fe, Co)O3-$_\delta$ system. For 20% Co compound, electrons (holes) were observed to move indirectly between Co ions via an O ion rather than directly between Co ions, i.e., the fluctuation of the charges of O ions as well as Co ion causes electrons (holes) to move with a complicated interaction between the generated holes and electrons. The effects of Fe doping in $La_{0.67}Sr_{0.33}CoO_3$ indicated that no apparent structure change was introduced by Fe doping up to x = 0.3, but the Curie temperature *Tc,* magnetization *M* and electrical resistivity are lowered by Fe substitution. A smaller localization length and a more severe disorder in the lattice due to Fe doping were observed. Previous research showed that two transitional metals, Fe and Co, at B site of ABO_3 allowed a better performance compared to only Co or Fe located at B site. For example, cobaltites exhibit a significant weight loss when the annealing temperature is higher 1000ºC (in some case 800ºC) and a higher resistivity and oxygen diffusivity were observed in ferrites.

The thermodynamic properties (stability and phase separation behavior) and total conductivity of prototype membrane materials were continued to be investigated. The data are needed together with the kinetic information to develop a complete model for the membrane transport. In previous studies, it was shown that iron based perovskite oxides show phase separation at intermediate partial pressures of oxygen, $-11 < \log pO_2 < -5$ at temperatures below 900 ºC.. Measurements on $La_{0.2}Sr_{0.8}Fe_{0.8}Cr_{0.2}O_{3-x}$ composition have proved difficult because of the difficulties in attaining equilibrium. Similar studies at 1000ºC suggested to temperature dependence due to some structural changes that are associated with cation rearrangements. The behavior was not seen with $La_{0.5}Sr_{0.5}FeO_{3-x}$ implying that B cation redistribution is the underlying cause. The B cation diffusion coefficients are much lower than for the oxygen ions and it appears likely that at the higher temperatures some slow rearrangement of the cations is occurring in response to the change in oxygen vacancy concentration. At lower temperatures, the B cation distribution is observed to be frozen in and the system responded only to the change in oxygen non-stoichiometry. Studies on isotope transients ($^{16}O_2$-$^{18}O_2$) on a second tubular membrane (6mm o.d., 1 mm wall thickness) of $La_{0.6}Sr_{0.4}Co_{0.2}Fe_{0.8}O_{3-\delta}$ (LSCF-6428) were also continued. Oxygen permeation measurements were made at temperatures between 1023K and 1123K. The isotopic transient is initiated by introducing an $^{18}O_2$ isotope pulse to the "air" (20%O_2 :Ar) side of the membrane while maintaining a constant pO_2. The isotopic composition of the oxygen permeate is analyzed on the delivery side, swept with helium, to reveal the residence time distribution of oxygen in the membrane under steady state transport. The resulting isotope transient allows the unambiguous separation of surface and bulk resistances to oxygen permeation under steady state conditions, a separation not possible by permeation measurements alone.

Task 1   Development of Ceramic Membrane/Metal Joints

**Prof. Thomas W. Eagar, Dr Harold R Larson,
Mr Raymundo Arroyave and Ms Jocelyn L. Wiese**

Experimental

Although relatively good high-contact area joints were obtained, in many cases such joints presented incipient micro-cracks precisely at the interface between the unaffected perovskite substrate and the 'reaction-affected' zone. It was obvious then that a way of minimizing the eventually detrimental interfacial reaction between the braze alloy and the perovskite substrate, an effective oxygen diffusion barrier was needed. Several diffusion barriers, based on stable oxides such as chromites, were deposited through PVD means were tried with unsatisfactory results.

Because of these results, further exploration of an effective diffusion barrier able to protect the perovskite membrane and at the same time easily bonded to a metallic part was necessary. Based on preliminary work on zirconia/metal joining performed in this group, an idea for a rather complex interfacial re-engineering of ceramic/metal seals started to emerge. The proposed new ceramic/metal interface, would consist of the usual perovskite substrate, coated with a dense zirconia layer, capable of protecting the rather unstable substrate from excessive reactions with the Ni-based brazing alloys:
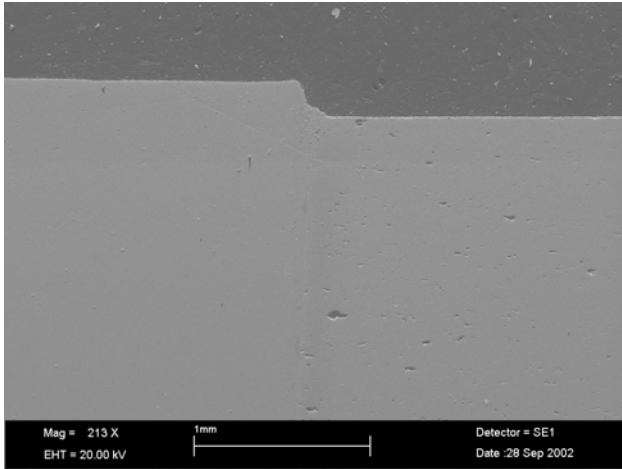

Super alloy

Ni Braze

Ti coating

Zirconia
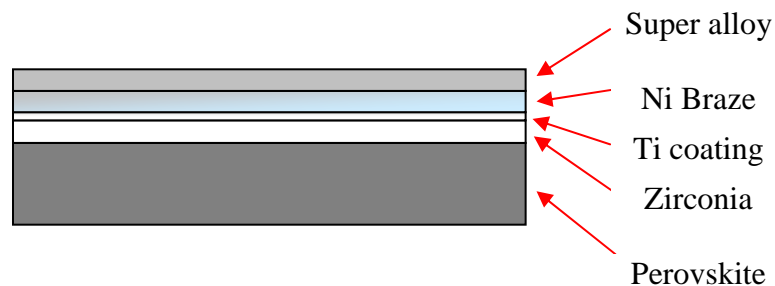
Perovskite

Figure 1 Interfacial Modification of Perovskite Membranes

Figure 1 illustrates the concept for a novel interface re-design that may eventually used to create reliable perovskite/metal brazed joints. One problem that has to be overcome when dealing with zirconia/metal joining applications is the fact that the zirconia surface is so stable that conventional liquid alloys usually do not wet it. Since wetting is essential for any practical liquid-based joining approach, the chemistry of the zirconia/liquid metal interface must thus be modified in order to promote wetting by the brazing alloy.

Results and Discussions

Because the ceramic/metal joint in question is intended to be used in high-temperature, oxidizing/reducing environments, the choice of possible brazing alloy families to be used was limited to Ni-based brazing alloys. Unfortunately, the usual approach of utilizing active element additions to conventional brazing alloys (adding Ti to Ag-Cu eutectic compositions) does not work in Ni-based brazing alloys due to the very strong thermochemical interaction between Ni and Ti in those brazes. Figure 1 illustrates a possible way to overcome this difficulty: by coating the zirconia sample with a thin layer of pure Ti metal, it is possible to metallize the surface. This active metallization in turn can promote wetting even on a very stable zirconia surface.

Figure 2 depicts a zirconia/Ni-based super alloy joint created using the process described above: A relatively thin Ti coating was deposited on top of the zirconia substrate and a Ni-based amorphous foil was placed between the coated zirconia sample and the Ni-based super alloy. The process was designed so at a relatively high temperature, the Ti coating would react with the zirconia and produce a Ti-based oxide that could in turn be wetted by the Ni-braze. Oxygen vacancies were created within the zirconia lattice and oxygen migration was promoted due to the large oxygen potential gradient across the zirconia/Ti interface. Once the Ti-oxide layer was formed, the joint was heated up until the solidus-liquidus two-phase region of the Ni-based braze alloy was reached. The liquid wetted the Ti oxide and a stable interface between the Ti-O coating and the Ni-based was created. As can be seen from the figure above, no interfacial defects were observed at the joint

Figure 2 Zirconia/Inconel Joint: Use of active coating and Ni-based super alloy

Conclusions

At this stage of the project, it would be desirable to have already concentric zirconia/metal joints. We have already prepared coated zirconia cylindrical samples and fabricated metallic cylindrical substrates to be joined to them. We have not finished the experiments yet but we expect to start making joints in a short period of time.

Attached to this report, we also enclose the paper presented in the 225th ACS Meeting in New Orleans, LA. In this paper, we summarize the main findings regarding the previously analyzed interfacial reaction between perovskite substrates and Ni-based super alloys.

We are also currently working on the final adjustments to thermochemical and kinetic models of ceramic/metal interfacial interactions under high-temperature conditions. It is expected that this work and the methodology developed will aid with the design of better ceramic/metal interfaces. Because of its importance as an effective protective coating for perovskite-based membranes to be brazed with Ni-based super alloys, the emphasis on this model development was on the understanding of the chemical interactions between zirconia substrates and active metal systems.

TASK 2: Determine material mechanical properties under conditions of high temperature and reactive atmosphere

Prof. Sukumar Bandopadhyay and Dr. Nagendra Nagabhushana

University of Alaska Fairbanks

EXPERIMENTAL PROCEDURE

Perovskites of the composition listed in Table 1, were acquired from Praxair Specialty Ceramics. The materials were processed by combustion spray pyrolysis. The average particle size 'd_{50}' was 0.6 μm. The materials were analyzed by X-ray to determine the lattice structure.

Green samples of dimension 50 x 6.7x 10 mm were fabricated by mixing with PVA as binder and cold pressing in a steel die at pressure of 28 MPa. The samples are to be sintered at 1350°C for 2-3 hours to the final density of ~ 90-95%. The samples processed will be evaluated for strength and characterized for crack growth in the environment.

Table 1: Composition of perovskite processed for flexure tests.

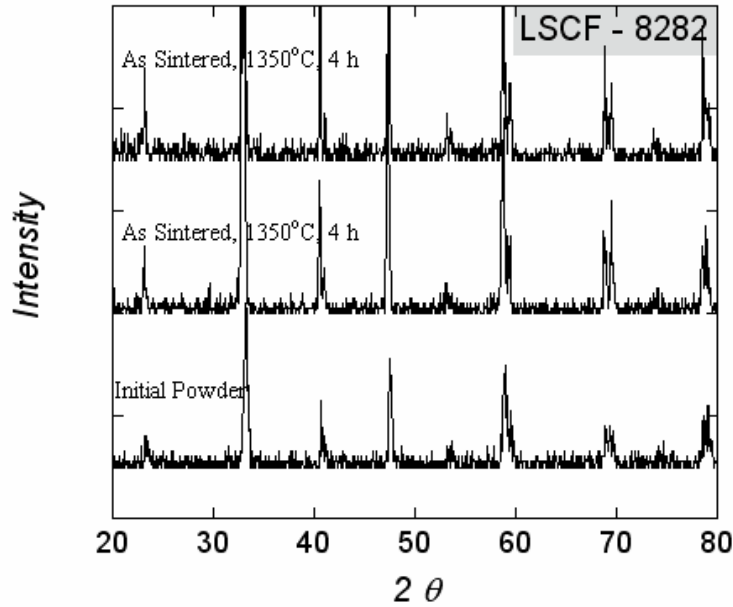| No.	Composition	Particle size d_{50}	Major Phase	Sintering Conditions	Sintered Density g/cc	Theoretical Density g/cc
1	LaSrFeO (LSF)	0.6	Perovskite	1250/4 h	6.66	
2	$La_{0.8}Sr_{0.2}CoO$ (LSC)	0.6	Perovskite	1250/4 h	6.3	
3	$La_{0.2}Sr_{0.8}Co_{0.8}Fe_{0.2}O_{3-\delta}$ (2882)	0.6	Perovskite	1250/4h	6.2 (?.)	
4	$La_{0.6}Sr_{0.4}Co_{0.2}Fe_{0.8}O_{3-\delta}$ (6428)	0.6	Perovskite	1300/4h	6.06	6.37
5	$La_{0.8}Sr_{0.2}Co_{0.8}Fe_{0.2}O_{3-\delta}$ (8282)	0.6	Perovskite	1350/4h	6.58	6.68

Fig 3: XRD analysis of LSCF- 8282 after sintering

The samples were analyzed in a XRD after sintering and characterized for porosity and final density before proceeding to mechanical strength as a function of environment. The samples will be thermally etched in air at 1150ºC for 0.5h for microstructure analysis. Previous studies on LSFCO membranes have indicated preferential segregation of cations upon exposure to environment and stress. For this reason, the membranes will be well characterized for segregation prior to exposure to the environment. One of the major questions that need to be addressed is environmental effects on crack initiation vs. crack propagation. For this the characterized membrane materials will be indented at various loads and along with a control sample, exposed to the environment of study. Post exposure and comparative studies (XRD, EDS and etc.) on existing and new indents would indicate the extent of cation segregation, decomposition of the perovskite and their influence on crack propagation. Similar studies on LSFCO would provide an excellent point of comparison with the well characterized LSCF (in terms of defect chemistry and stability).

Hardness and Fracture Toughness:

The hardness and fracture toughness of the membrane materials are being determined. The samples were mounted and polished to 0.25μm finish. The Vickers hardness (*H*) and the fracture toughness (*K_c*) were measured by applying varying loads (.98 N – 9.8 N) for 15 s. The diameters and crack lengths of five indents (at each load) in each material were evaluated using the formula:

$$K_c = 0.032 H a^{\frac{1}{2}} \left(\frac{E}{H} \right)^{\frac{1}{2}} \left(\frac{l+a}{a} \right)^{\frac{-3}{2}}$$

Where *2a* is the indent diameter and *l* is the crack length measured from the indent tip to the crack tip

A typical micrograph of the indent with lateral cracks extending from the tips of the indent is shown in figure 4.
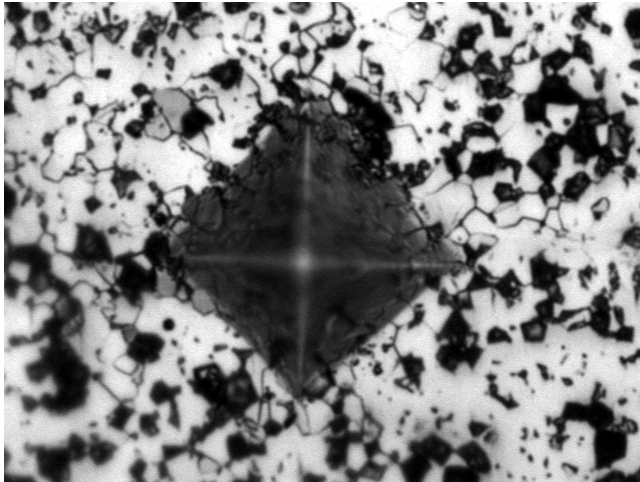

Fig. 4: Vickers indents on
LSCF – 8282 for
fracture toughness
and crack growth
studies

.

Task 3:   Preparation and Characterization of Dense Ceramic oxygen Permeable Membranes

By: Professor Harlan Anderson, University of Missouri-Rolla
Dr. Wayne Huebner, Dr. Xiao-Dong Zhou

INTRODUCTION[*]

The perovskite-type oxides encompass a large variety of chemical compositions that contribute to their diverse and unique properties. Of them, $La_{1-x}Sr_xFeO_{3-\delta}$ is of particular interest in the applications of gas separation membrane, mixed ionic and electronic conductors and solid oxide fuel cells because of their special structural, electric and magnetic properties. Dann et al.[1] have reported the orthorhombic phase for $0 ¡Ü x ¡Ü 0.2$, the rhombohedral phase for $0.4 ¡Ü x ¡Ü 0.7$ and the cubic phase for $0.8 ¡Ü x ¡Ü 1.0$. Nèel temperatures of this series compounds were measured by Shimony et al.[2] with values from 750K to about 100K as x changes from 0 to 1 and around 300K when x = 0.4. It is the intent of this report to summarize the studies over FY 2002 on the ferrites, with an emphasis on the compound of $La_{0.6}Sr_{0.4}FeO_{3-\delta}$, which is particularly interesting in the applications for use as oxygen membranes and as the cathode for intermediate temperature solid oxide fuel cells (SOFCs). Most of the studies have been focused on the SOFC applications, but the results are applicable to oxygen separation as well. Recently, $La_{0.8}Sr_{0.2}FeO_3$ has been demonstrated at Pacific Northwestern National Lab as a better cathode in SOFCs at relatively low operation temperature (750°C) than $La(Ni, Fe)O_3$ and $(La, Sr)(Ni, Fe)O_3$ 3. Initial studies on both separation membranes and SOFCs in our group on ferrite materials have shown that the structure plays an important role in electrical and catalytic properties and that the electrical, catalytic and magnetic properties have an inter-relationship that is commonly related to the electronic structure and oxygen vacancy concentration (See appendices). Therefore, it is critical to study the ferrite materials from the atomic structure point of view, for example the hybridization of transitional metal and oxygen orbitals that plays a dominant role in the properties such as the generation of oxygen vacancies, holes, and spin state of the transitional metals. This interrelationship is shown in the $(La, Sr)(Fe, Co)O_{3-\delta}$ system. For 20% Co compound, electrons (holes) move indirectly between Co ions via an O ion rather than directly

---

[*] This is a manuscript drift version we will submit for publishing with the co-authors as Z. Chu, W. B. Yelon, J. Yang, W. J. James, and Q. Cai.

between Co ions, i.e., the fluctuation of the charges of O ions as well as Co ion causes electrons (holes) to move with a complicated interaction between the generated holes and electrons [4]. The effects of Fe doping in $La_{0.67}Sr_{0.33}CoO_3$[5] showed that no apparent structure change was introduced by Fe doping up to x = 0.3, but the Curie temperature *Tc,* magnetization *M* and electrical resistivity are lowered by Fe substitution. A smaller localization length and a more severe disorder in the lattice due to Fe doping were observed. Previous research showed that two transitional metals, Fe and Co, at B site of ABO_3 allowed a better performance compared to only Co or Fe located at B site. For example, cobaltites exhibit a significant weight loss when the annealing temperature is higher 1000ºC (in some case 800ºC) and a higher resistivity and oxygen diffusivity were observed in ferrites.

EXPERIMENTAL

The Pechini method[6, 7] was used to synthesize nanocrystalline particles, in this process a polymeric solution was formed due to a chelating reaction between cations and chelants. The polymeric solutions were also used as the thin film sources, which were used to fabricate thin films by spin coating and thermal processing. Electrical conductivity was measured by the four-probe method at the temperature from 150 – 1000ºC in a wide range of oxygen activities (10^{-25} to

1). Thermogravimetric analysis was conducted at 1000 and 1200ºC in O_2, air and Ar. Mössbauer spectroscopy and neutron diffraction were performed at room temperature on the sintered and quenched specimens. During the quenching experiments, the specimens were first heated at 1000°C with a flowing gas atmosphere of N_2, air, or CO/CO_2 mixtures for 24 hours, and then quenched to room temperature. For Neutron Diffraction (ND) studies, samples were contained in 3 mm V metal cells and data were collected at 1.4785 Å over a range of 5º-105º (2è). Rietveld refinement was carried out using the FULLPROF code, in which the magnetic ordering was taken into account because of the sensitivity of neutron diffraction to the magnetic ordering of the Fe atoms.

RESULTS

Figure 5 shows powder Neutron Diffraction Patterns of $La_{0.6}Sr_{0.4}FeO_{3-\delta}$ quenched at various gas environments. The powder Neutron Diffraction results showed that all specimens were single phase with an exception of the sample quenched with $90\%CO/10\%CO_2$, in which peak broadening and asymmetry took place that indicated a decomposition of the sample. Four models were used to fit the data for each sample and all results seemed reasonable. However, there did exist different preferred models for the reduced samples than for the air- and N_2- quenched samples and the neutron diffraction patterns for the samples quenched from the reducing atmosphere are significantly different with those quenched from air or N_2. The diffraction peak splitting for the reduced samples is dramatically reduced compared to the N_2- and air- treated samples. The first diffraction peak (~ 19°) is much stronger in the reduced samples than in the air- or N_2- quenched samples. This peak proves to be purely magnetic and the change reflects a large increase in magnetic moment for the reduced samples vis-à-vis the air- and N_2- quenched samples.
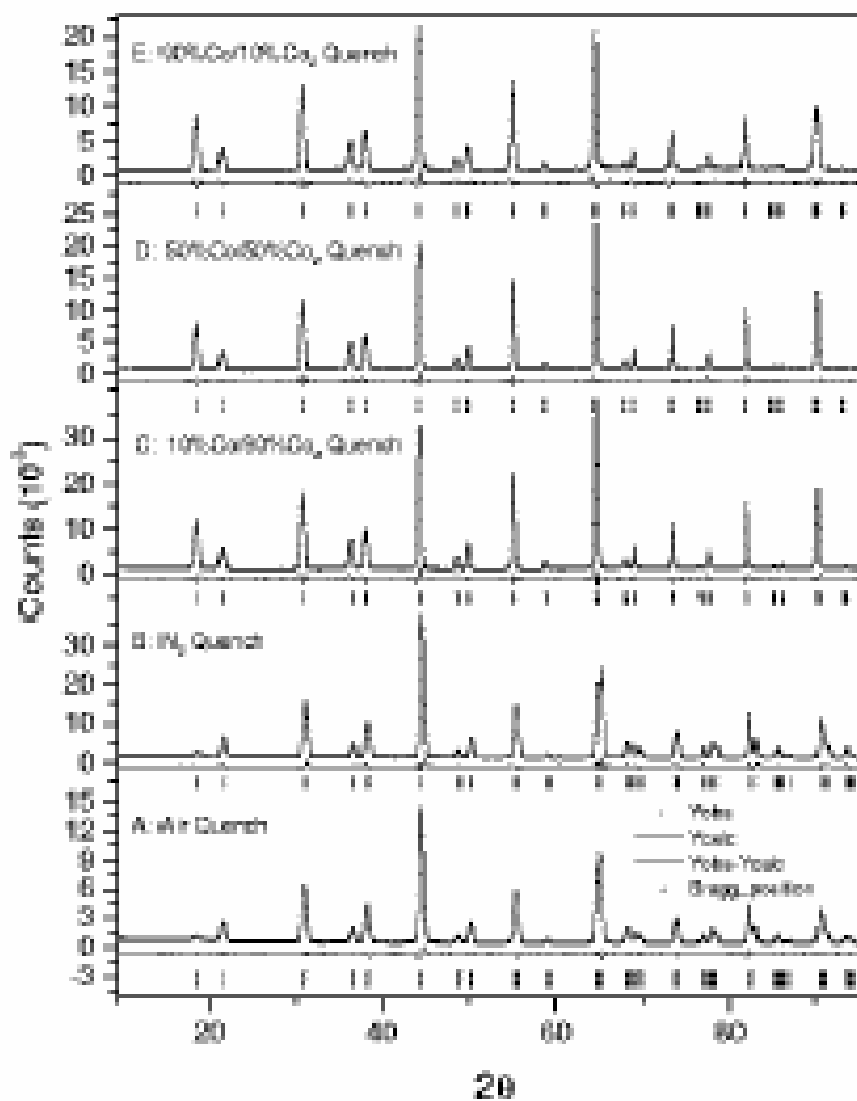
Figure 5. Powder Neutron Diffraction patterns of $La_{0.6}Sr_{0.4}FeO_{3-\delta}$ quenched at various gas environments.

Further study was then performed on the electrical conductivity of $La_{0.6}Sr_{0.4}FeO_{3-\delta}$ at the low pO_2, in which oxygen vacancy concentrations were increased. Figure 7 shows the plot of $\log(\sigma)$ vs. $\log(pO_2)$ at 1000°C with a control over the oxygen activity being made by using a mixture of CO/CO_2, from which the pO_2 can be determined thermodynamically. In Figure 3, a transition from p-type to n-type of conductor is obvious at relative low pO_2, at which the majority carriers changed from the holes to electrons because of the valence state decreases in Fe due to the further loss of oxygen. The oxygen vacancies are generated at high temperature due to loss of

15

oxygen, which results in a higher oxygen vacancy concentration and a lower hole concentration. In addition to the conductivity, oxygen vacancy concentration also plays a key role in the function of cathodes, in particular in the catalytic properties. Determination of the oxygen vacancy level has been performed by thermogravimetric analysis (TGA) and neutron diffraction. TGA simply measures the weight changes with the variable being time, gas environment and temperatures. Neutron diffraction was performed on the samples which were quenched at 1000ºC from different oxygen activities. A large decrease in 3-δ was observed when the was gas changed from 90%CO to 99%CO. XRD results showed that $La_{0.6}Sr_{0.4}FeO_{3-\delta}$ decomposed in the 99% CO atmosphere. The consistence results between TGA and neutron diffraction confirmed that the quenching experiment could be used to study the ferrites under reducing conditions.
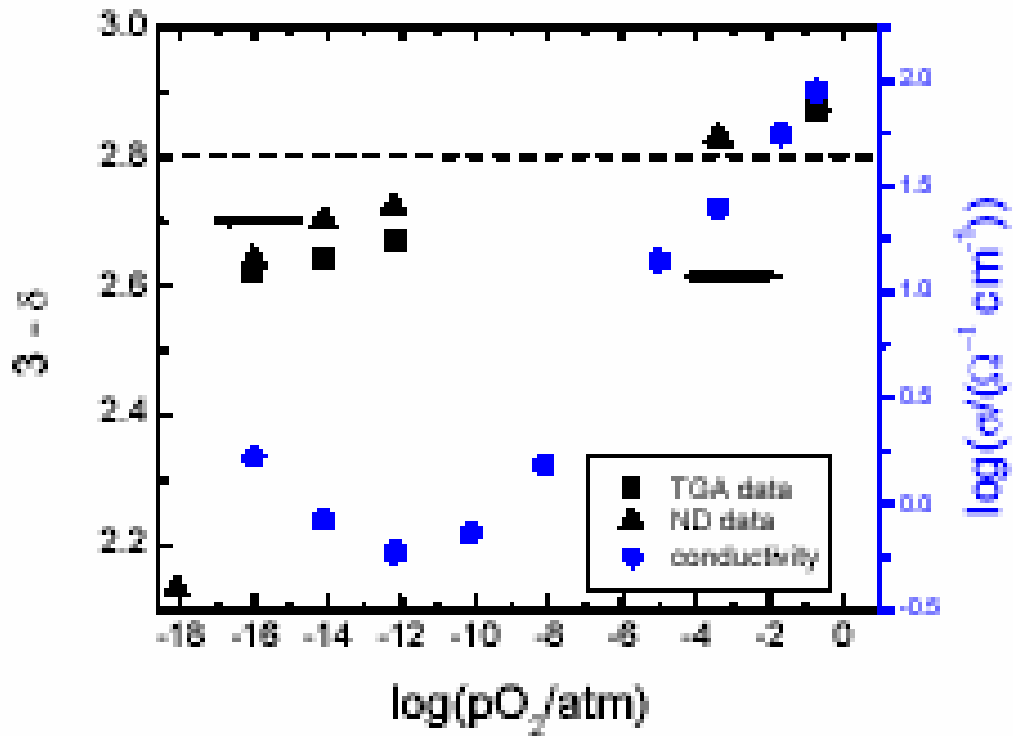
Figure 6. Log(σ) and 3-δ as a function of log(pO2) for $La_{0.6}Sr_{0.4}FeO_{3-\delta}$

.

Further study was then performed on the electrical conductivity of $La_{0.6}Sr_{0.4}FeO_{3-\delta}$ at the low pO2, in which oxygen vacancy concentrations were increased. Figure 6 shows the plot of log(σ) vs. log(pO2) at 1000ºC with a control over the oxygen activity being made by using a mixture of CO/CO2, from which the pO2 can be determined thermodynamically. In addition to the conductivity, oxygen vacancy concentration also plays a key role in the function of cathodes, in particular in the catalytic properties. Determination of the oxygen vacancy level has been performed by thermogravimetric analysis (TGA) and neutron diffraction. TGA simply measures the weight changes with the variable being time, gas environment and temperatures. Neutron diffraction was performed on the samples, which were quenched at 1000ºC from different oxygen activities. A large decrease in 3-δ was observed when the gas was changed from 90%CO to 99% CO. XRD results showed that $La_{0.60}Sr_{0.40}FeO_{3-\delta}$ decomposed in the 99% CO atmosphere.

CONCLUSIONS

The consistence results between TGA and neutron diffraction confirmed that the quenching experiment could be used to study the ferrites under reducing conditions. Figure 7 shows a relative high oxygen vacancy level in ferrites over a wide oxygen activity, whereas, LSM only exhibits sufficient oxygen vacancy concentration in the lower oxygen activity region [8].
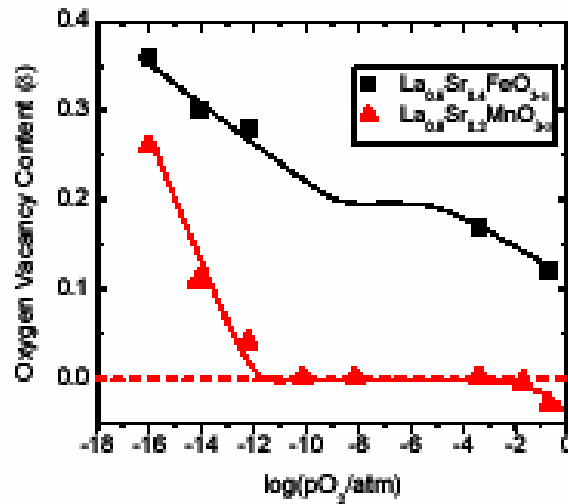

Figure 3: Oxygen content (3-δ) vs. log(pO$_2$) for La$_{0.6}$Sr$_{0.4}$FeO$_{3-\delta}$ and La$_{0.8}$Sr$_{0.2}$MnO$_{3-\delta}$ [8] at 1000°C.

Figure 8 shows Nèel Temperature and Fe-O-Fe angles as a function of pO$_2$, at which the specimen was quenched. The bonding angles of Fe-O-Fe were increased with decreasing oxygen partial pressures. Because the bonding lengths were nearly constant, the increasing of the bonding angle increases the overlap between Fe and O atomic states

18

that results in an increase in the superexchange interaction between Fe and Fe. The Fe-Fe super-exchange interaction is highly dependent on the Fe-O-Fe bond angle and the superexchange through the oxygen atoms that is more effective when the Fe-O-Fe paths are close to linear [9, 10]. It is also found that the increase in the superexchange interaction results in an increase in Nèel temperature, as shown in Figure 3. The Fe moments for the three reduced samples refine between 3.72 and 3.82 μ_B while the moments for the other two samples are much smaller (1.4 μ_B and 1.2 μ_B for the air- and N_2- quenched samples, respectively).

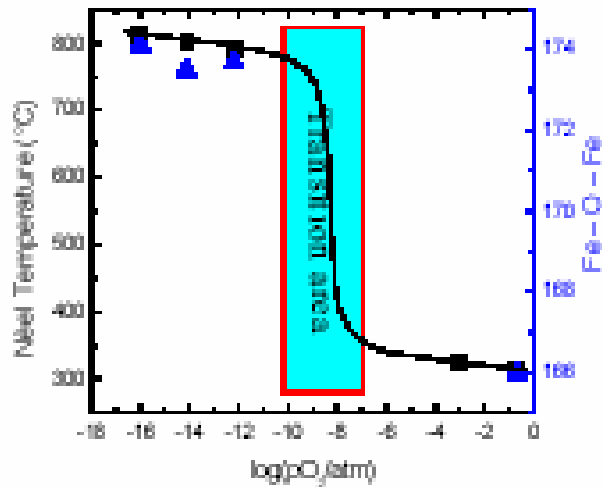Figure 4. Nèel temperature and Fe – O – Fe angle of the specimens quenched at various oxygen partial pressures (pO_2).

TASK 4:   Assessment of Microstructure of the Membrane Materials to Evaluate the Effects of vacancy-Impurity Association, defect Clusters, and Vacancy Dopant Association on the Membrane Performance and Stability

Professor Nigel Browning, University of Illinois Chicago Circle

After the over one year break in funding for the UIC section of the research project, this quarter's research has focused on the training of a new graduate student to perform the analysis of membrane materials.   Following the guidance that was received from the other project participants at the meeting in Rolla, the analysis will focus on the identification of precipitates at grain boundaries in fracture surfaces produced during testing at UAF. Of key importance in identifying the reasons for mechanical failure will be determining whether precipitation is a function of the deformation itself or produced in fracturing the surfaces. Initial analysis during this quarter's research has determined mechanisms of specimen preparation that will permit grain boundaries to be analyzed. The first quarter of 2003 will be spent performing initial analyses in the microscope to study the composition and distribution of precipitates at grain boundaries.

Task 5:   Measurement of Surface Activation/Reaction rates in Ion Transport Membranes using Isotope Tracer and Transient Kinetic Techniques.

Prof. Alan Jacobson, University of Houston/University of Toronto

University of Houston

EXPERIMENTAL

Because of problem as encountered in previous reports, we have repeated the original series of measurements with longer equilibration times. The measurements were made on a powdered sample by coulometric titration in a sealed electrochemical cell with a YSZ pump and a YSZ sensor to monitor the internal pO_2 and the approach to equilibrium. The apparatus has been described in previous reports. Isotherms have been measured at 750, 800, 850, 900, 950, 1000, and 1040 ºC. The data for two temperatures, 850 and 1000 ºC, are shown in Figure 1 as representative examples.
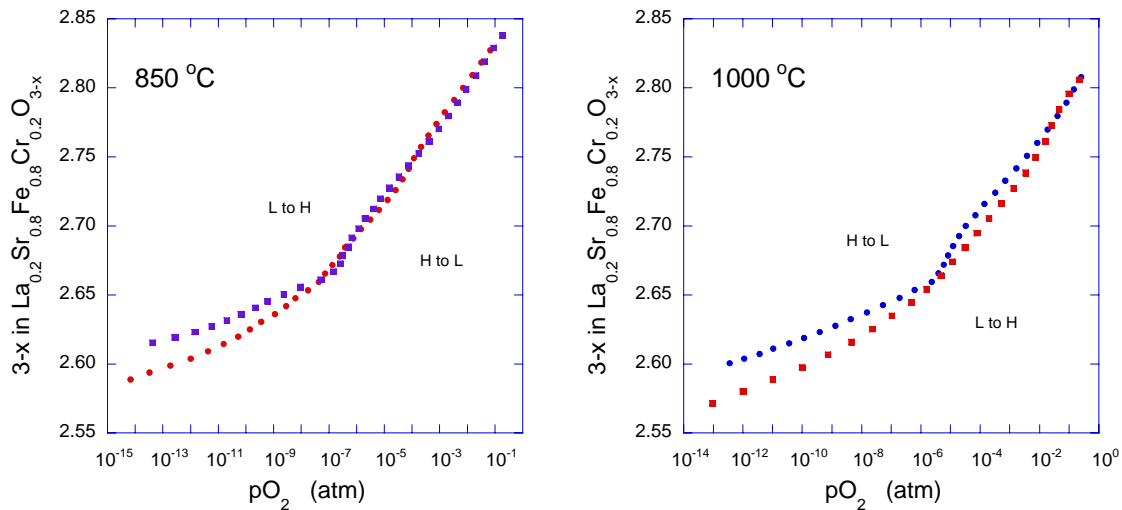

Figure 9. Variation of the oxygen stoichiometry in $La_{0.2}Sr_{0.8}Fe_{0.8}Cr_{0.2}O_{3-x}$ as a function of oxygen partial pressure at 850 and 1000 ºC.

RESULTS AND DISCUSSIONS

The data in each case were measured on increasing (L to H) and decreasing (H to L) the oxygen partial pressure. The data obtained at 850 ºC show that the stoichiometry varies from ~2.85 to 2.6 over the pressure range studied. From the stoichiometry $La_{0.2}Sr_{0.8}Fe_{0.8}Cr_{0.2}O_{3-x}$ a

lower limit of 2.6 corresponding to the reduction of all Fe^{4+} to Fe^{3+} and no reduction of Cr^{3+} is expected. The absolute values of the stoichiometry were obtained by normalizing to a reference value determined by chemical titration. The uncertainty in 3-x is ±0.05.

The data at 850 ºC, show good agreement between measurements on increasing and decreasing pO_2 above 10^{-7} atm. Close to $pO_2 = 10^{-7}$ atm, a discontinuity is apparent in the data that is more pronounced in the results obtained on increasing pO_2. Below this partial pressure, equilibrium is not achieved and the results obtained in the two different measuring directions differ by an increasing amount with decreasing pO_2. The general behavior of the data at 1000 ºC is similar, a discontinuity is again apparent though it is now at ~10^{-6} atm and equilibrium is not achieved at the lower partial pressures. Furthermore, even for the higher partial pressure data ($pO_2 > 10^{-6}$ atm) the results obtained in the two measurement directions do not agree perfectly. In general, the apparent non-equilibrium behavior becomes more pronounced at higher temperatures and is greater at lower pressures below the discontinuity.

The temperature dependence suggests that some structural changes occur that are associated with cation rearrangements. The behavior is not seen with $La_{0.5}Sr_{0.5}FeO_{3-x}$ implying that B cation redistribution is the underlying cause. The B cation diffusion coefficients are much lower than for the oxygen ions and it appears likely that at the higher temperatures some slow rearrangement of the cations is occurring in response to the change in oxygen vacancy concentration. At lower temperatures, the B cation distribution is frozen in and the system responds only to the change in oxygen non-stoichiometry. The presence of the discontinuity at 10^{-6} to 10^{-7} suggests an intermediate phase with some composition width.
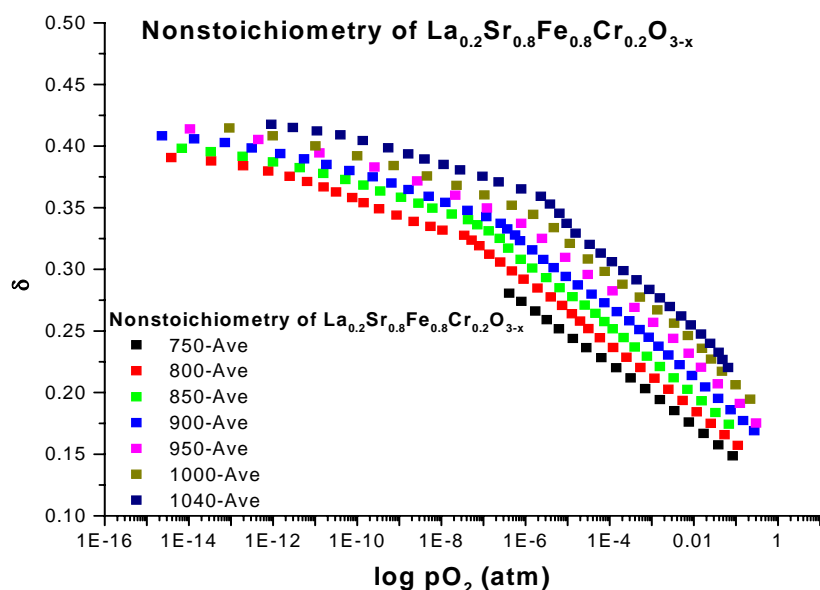
Figure 10. The average values of the non-stoichiometry of $La_{0.2}Sr_{0.8}Fe_{0.8}Cr_{0.2}O_{3-x}$.

The hysteresis in the stoichiometry at low pO_2 is associated with crossing this two-phase region or at high temperature, a region where considerable short-range order persists. In Figure 10, the average values of the non-stoichiometry for the seven isotherms are displayed. Because of the equilibrium problem, at low pO_2 the uncertainty is large and increases with temperature ($\pm$ 0.02 at 1040 ℃). The data obtained on increasing and decreasing pO_2, in the equilibrium range ($>10^{-8}$ atm), were averaged and fit, in order to extract the temperature dependence of the stoichiometry at different pO_2s. The interpolated results are shown in Figure 11 as isobars at $\log(pO_2)$ increments of -1 from 0 to -8. The dotted line indicates the position of the phase boundary.
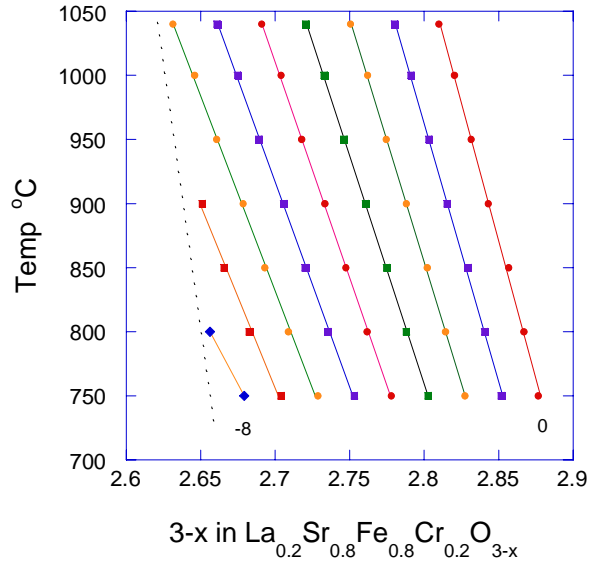
Figure 11. The phase diagram of $La_{0.2}Sr_{0.8}Fe_{0.8}Cr_{0.2}O_{3-x}$.

Also, in this quarter, tubular ceramic samples of $La_{0.2}Sr_{0.8}Fe_{0.8}Cr_{0.2}O_{3-x}$ were cut and polished to fit the transient membrane reactor at UT.

Plans for next quarter.

We will begin a series of measurements on a new composition that has been selected by Praxair. Initially, we will characterize the materials by X-ray powder diffraction and by electron probe microanalysis. We will then investigate the densification of the material in order to prepare dense ceramics for dc conductivity measurements and tubular ceramics for use in the membrane reactor at UT.

University of Toronto

Isotope Transient Studies of Oxygen Permeation Through a Dense La$_{0.6}$Sr$_{0.4}$Co$_{0.2}$Fe$_{0.8}$O$_{3-\delta}$ Membrane

EXPERIMENTAL

The apparatus as described in previous reports is shown again in Figure 12 for reference. The transients obtained on the previous membrane showed that both surface exchange and bulk transport resistances contribute significantly to membrane performance. A dispersion flow model was used to fit the data and provide values of the individual transport parameters (forward and reverse surface exchange rate coefficients as well as the oxygen diffusion coefficients).

During the past 3 months, we have placed another membrane of LSCF-6428 in the reactor in order to complete some key experiments. The first was destroyed by hydrocarbon introduction to the flow system. The new membrane behaves similarly to the previous one. The main experiments to be performed on this second membrane are:

(1) *Isotope transients at various He sweep rates.* Variation in the He sweep rate produces variations in the oxygen partial pressure on the delivery side, and hence affects the driving force across the membrane. The flux changes as a result. Isotope transients performed at different He sweep rates will reveal how the operating membrane responds to the larger driving force.

(2) *Briefly investigate of the effect of water:* Isotope transients will be performed with substantial water partial pressure on the air side. Any differences in flux will be investigaged by isotope transients to see if the effect is surface or bulk related.

(3) *Performance of a "quench" experiment:* The membrane will be cooled during an isotopic transient, thus freezing the isotope distribution in the material during the evolution of the transient. The membrane will then be cut and the internal isotope distribution measured by SIMS. This will provide a rigorous test of the model. It will reveal any radial and axial inhomogeneities in the flow of oxygen through the membrane. It may also provide evidence of changes in the diffusion coefficient with position.

25

RESULTS AND DISCUSSIONS

We have made progress in the first of these objectives during the last quarter. Figure 13 shows that, like the first membrane, the oxygen flux through this membrane does depend on the He sweep rate (pO_2 difference).

Isotope transients were performed at He sweep rates of 20 and 60 mL/min. The resulting isotope transients are shown in Figure 14. Clearly the change in flux and oxygen activity driving force produced a change in the oxygen residence time distribution in the membrane. At the higher He sweep rate, the larger flux speeds up the appearance of isotope on the delivery side, makes the surface exchange rates less reversible and sharpens up the shape of the transient in a manner consistent with a smaller degree of dispersion due to diffusion. We are currently modeling these results to reveal which of the transport properties, including the reversibility of the surface activation rate, were altered the most by this change in operating conditions.

We have also added to the quality of these transients by monitoring the "back exchange" of ^{18}O on the air-side after the pulse of isotope. This back exchange provides a check on our derived values of the reversibility of the oxygen activation reaction. Figure 15 shows the back exchange under two different conditions. At 850°C, the back exchange is more extensive than at 800°C. This effect arises from a combination of the larger flux which places more isotope in the membrane as well as the faster surface exchange rates. We are currently modeling these results to derive more reliable surface exchange rates.

Finally, we have received from Houston a tube made of $La_{0.2}Sr_{0.8}Cr_{0.2}Fe_{0.8}O_{3-\delta}$ which we have successfully prepared for use in isotope transient experiments under synthesis gas production conditions.

PLANS:

We will finish objectives 2 and 3 from the list above and model the results. We will then install the recently received $La_{0.2}Sr_{0.8}Cr_{0.2}Fe_{0.8}O_{3-\delta}$ membrane. The initial experimental program on this material will follow the program below:

(1) Initial flux measurements will be made with He sweep and isotope transients performed in an air separation mode.

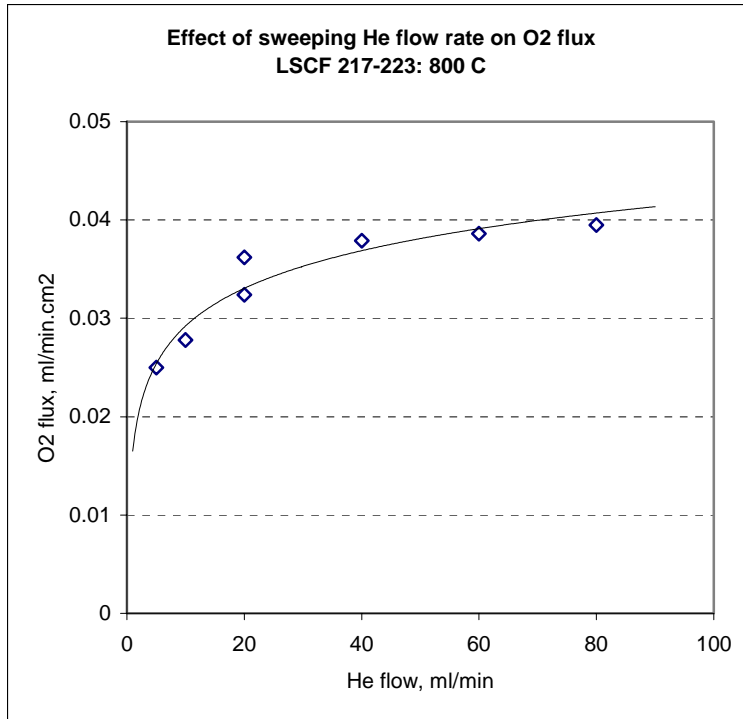(2) Establishment of synthesis gas atmospheres will allow oxygen transport rates under syngas conditions.

(3) Isotope transients under the large gradient conditions will be obtained and compared to those under air separation conditions.
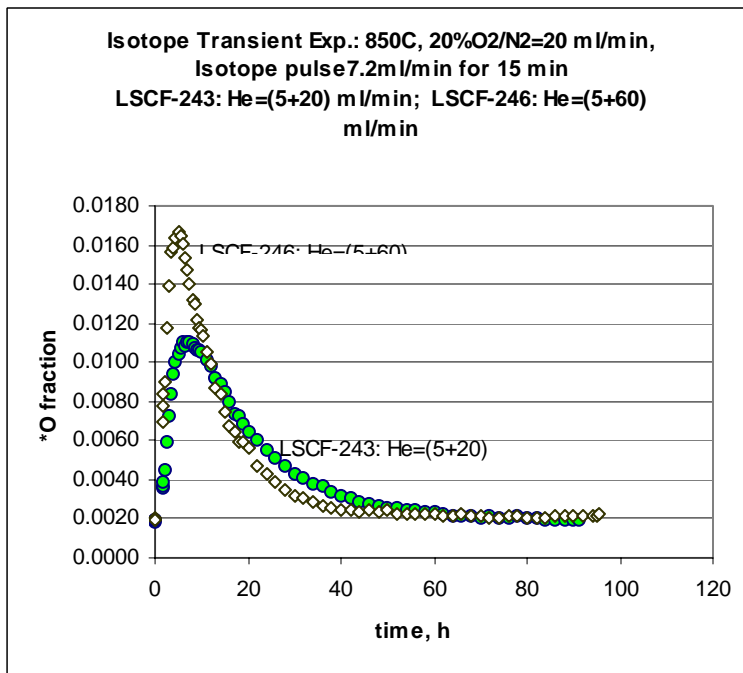
TORONTO FIGURES:
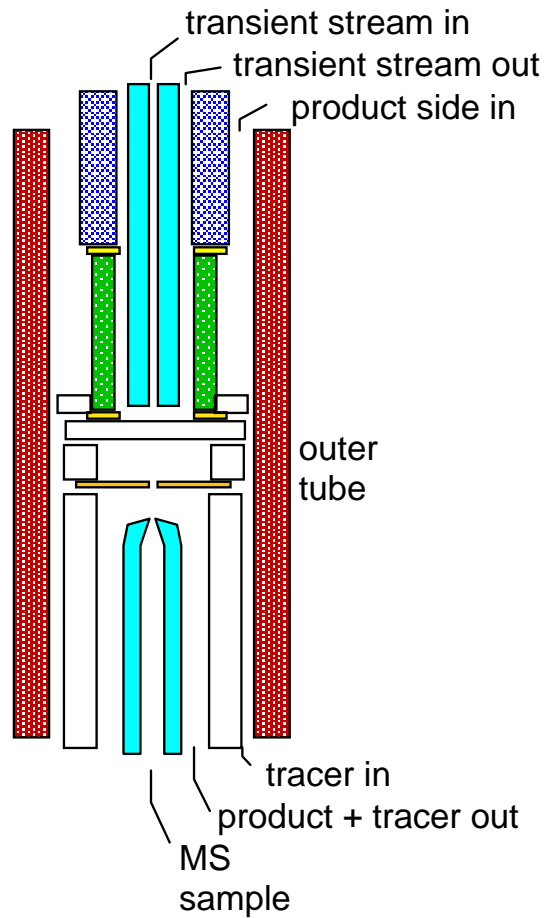
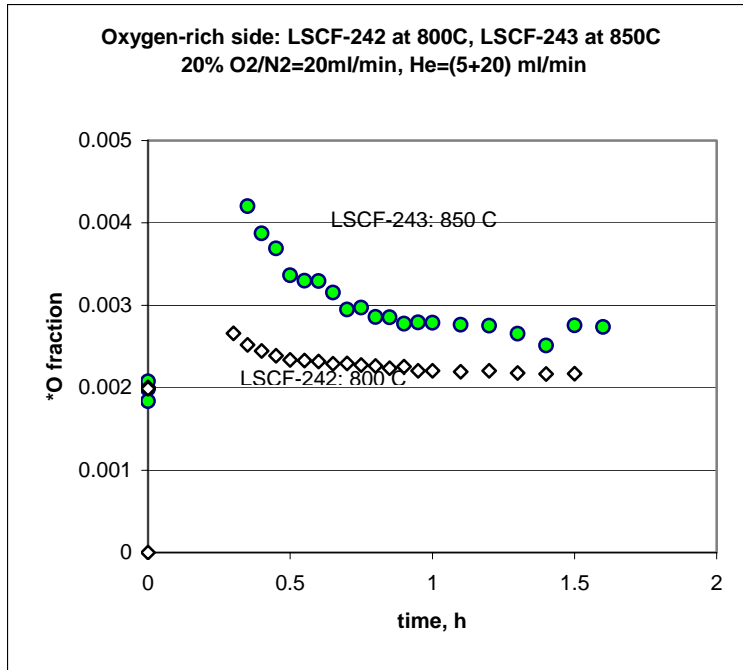**Figure 12: Schematic of the isotope transient experimental reactor.**

Figure 13: Oxygen flux in mL(STP) min⁻¹ cm⁻² as a function of He sweep rate on the delivery side at 800°C.

Figure 14: ¹⁸O isotope transient on LSCFO membrane at two different He flow rates at 850°C.

Figure 15: The isotopic response (back exchange) on the air side of a LSCFO membrane after an ^{18}O isotope pulse. Data are shown for two temperatures.

CONCLUSIONS

Current thermochemical and kinetic models will aid the design of better ceramic/metal interfaces. Because of its importance as an effective protective coating for perovskite-based membranes to be brazed with Ni-based super alloys, the emphasis on this model development is on furthering the understanding of the chemical interactions between Zirconia substrates and active metal systems.

The Fe-Fe super-exchange interaction is highly dependent on the Fe-O-Fe bond angle and the superexchange through the oxygen atoms is more effective when the Fe-O-Fe paths are close to linear. The increase in the superexchange interaction results in an increase in Nèel temperature and the Fe moments for the three reduced samples refine between 3.72 and 3.82 μ_B while the moments for the other two samples are much smaller (1.4 μ_B and 1.2 μ_B for the air- and N_2-quenched samples, respectively).

Initial flux measurements $La_{0.2}Sr_{0.8}Cr_{0.2}Fe_{0.8}O_{3-\delta}$ membrane were made with He sweep and isotope transients performed in an air separation mode. Isotope transients under the large gradient conditions need to be obtained and compared to those under air separation conditions

REFERENCES:

1. S. E. Dann, D. B. Currie, and M. T. Weller, *J. Solid State Chem.,* **109**, 134 (1994).

2. U. Shimony and J. M. Knudsen, *Phys. Rev.*, **144**, 361 (1966).

3. S. P. Simner, J. F. Bonnett, N. L. Canfield, K. D. Meinhardt, V. L. Sprenkle, and J. W. Stevenson, *Electrochem. Solid State Lett.*, **5**, A173 (2002).

4. Takahashi, H.; Munakata, F.; and Yamanaka, M. *Phys. Rev. B.* **1998**, *57,* 15211.

5. Sun, Y.; Xu, X.; Zhang, Y. *Phys. Rev. B.* **2000**, *62*, 5289.

6. Pechini, M., U.S. Pat., No. 3,330,697, **1967**

7. Anderson, H. U., Chen, C.-C., and Nasrallah, M. N., U.S. Pat., No. 5,494,700, **1996**.

8. J. H. Kuo, H. U. Anderson and D. M. Sparlin, *J. Solid State Chem,* **83**, 52 (1989)

9. Chu, Zili, University of Missouri-Columbia, Dissertation, **2002.**

10. Goodenough, J. B., Magnetism and Chemical Bond, Edited by F. A. Cotton (Interscience Publishers, London, 1976) Vol. 1, p. 170

BIBLIOGRAPHY:

N/A

LISTS OF ACRONYMS AND ABBREVIATIONS:

N/A